CHEMISTRY
A EUROPEAN JOURNAL

COMMUNICATION

DOI: 10.1002/chem.201201646

Early Stages of Oriented Attachment: Formation of Twin ZnO Nanorods under Microwave Irradiation

Monica Distaso,*[a] Mirza Mačković,[b] Erdmann Spiecker,[b] and Wolfgang Peukert[a]

Nonclassical crystallization represents a unique tool to fabricate ordered superstructures. The underlying oriented attachment mechanism (OAM) implies the spontaneous assembly of building blocks with common crystallographic orientations.[1] The driving force is the reduction of the surface free energy by eliminating the high-energy facets, but the detailed mechanisms are still not clear.[2]

In the framework of our interest for the synthesis of complex nanostructures, we have recently reported that ZnO mesocrystals can be synthesized under solvothermal conditions in the presence of poly-*N*-vinyl-pyrrolidone (PVP), and that the polymer matrix plays a key role as directing agent during the synthesis.[3]

ZnO in wurtzite phase is constructed by a number of alternating planes stacked along *c* axis direction giving a Zn^{2+} (0001) and O^{2-} (000−1) terminated faces. ZnO is able to form twin structures, that is, crystals in which facets with the same polarity are coupled to form a single crystal with various morphologies.[4–9]

According to the state of the art, the twinning process can be promoted by inorganic[10] or polymeric[11] species adsorbed onto the coupling interfaces. Bioinspired synthesis provide an additional tool for studying the nature of the interfaces and forces involved during oriented attachment.[12]

Herein, we showed that in water and under microwave (MW) irradiation, ZnO nanorods with a characteristic seam cut perpendicular to the elongation direction form (Figure 1). Scanning electron microscopy (SEM) analysis of the as-obtained particles showed that the sample consists of rods with hexagonal cross-section with a length between 320 nm and 2.5 μm and a width of 71–367 nm with an aspect-ratio (AR) distribution between two and ten (Figure 1).

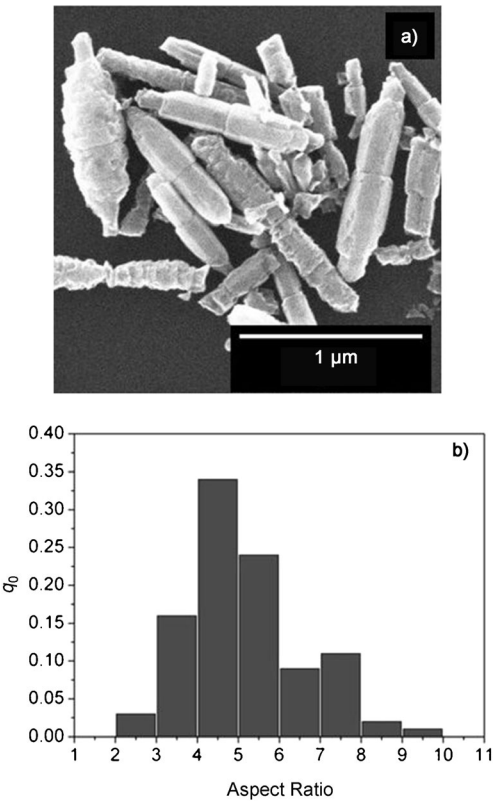

Figure 1. a) SEM image of ZnO nanorods after 16 min of irradiation under MW; b) AR distribution of particles, in which $q_0 = [\Delta(\mathrm{AR})$ in interval between AR_i and $\mathrm{AR}_{i+1}]$/[total amount of rods × interval width $(\mathrm{AR}_{i+1} - \mathrm{AR}_i)]$.

Transmission electron microscopy (TEM) analysis and selected-area electron diffraction (SAED) of the sample isolated after 16 min showed that the interface between two ZnO rod parts is single crystalline and that the growth took place through *c* axis ([0001] direction; Figure 2a and corresponding inset). XRD evidenced that the final particles crystallized in wurtzite phase (Figure 2b), as was confirmed by SAED analysis (Figure 2a).

Kinetic measurements have been carried out with the aim to highlight the formation mechanism through the isolation of intermediate species. Thus, the reaction was repeated and stopped after 45 seconds, one, and two minutes, when the temperature inside the reaction mixture was 45, 58, and 153 °C, respectively. After 45 seconds, no precipitate formed,

[a] Dr. M. Distaso, Prof. W. Peukert
Institute of Particle Technology
FAU Erlangen Nürnberg, Cauerstrasse 4
91058 Erlangen (Germany)
Fax: (+49) 913-185-29401
E-mail: M.Distaso@lfg.uni-erlangen.de

[b] Dr. M. Mačković, Prof. E. Spiecker
Centre for Nanoanalysis and Electron Microscopy (CENEM)
Department of Materials Science and Engineering
FAU Erlangen Nürnberg
Cauerstrasse 6, 91058 Erlangen (Germany)

Supporting information for this article is available on the WWW under http://dx.doi.org/10.1002/chem.201201646.

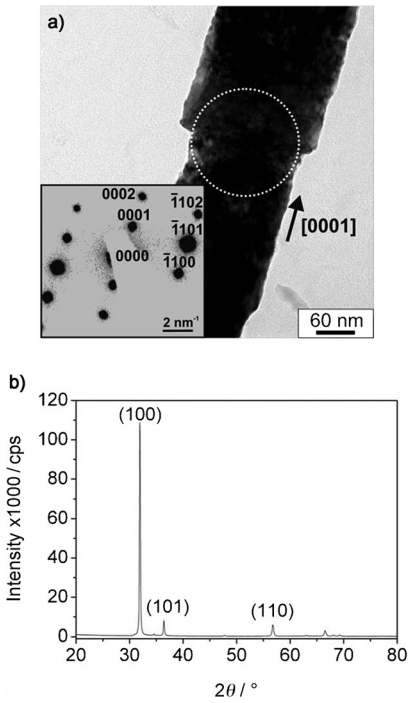

Figure 2. a) Bright-field TEM image of a ZnO nanorod and SAED pattern (inset in a) obtained at the seam cut (marked with the dotted circle), valid for the [110] zone axis of hexagonal ZnO (ICSD 26170). The SAED pattern is depicted in correct relative orientation to the TEM image and confirms that the long axis of the ZnO nanorod is parallel to the crystallographic [0001] direction; b) XRD of the final twin rods (16 min).

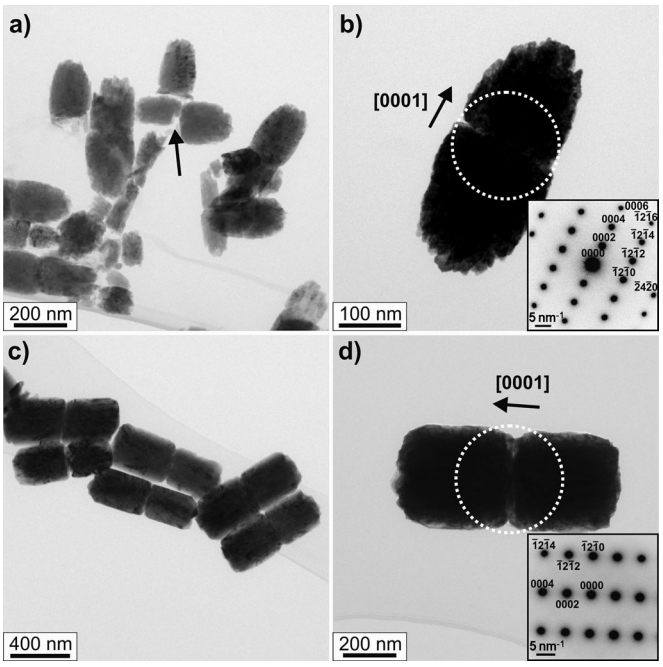

Figure 3. Bright-field TEM images of ZnO nanorods isolated after a reaction time of: a), b) 1 min; c), d) 2 min. The corresponding SAED pattern (insets in b and d) were obtained at the interface between the rod parts (marked with the dotted circles) and are valid for the [210] zone axis of hexagonal ZnO (ICSD 26170). Both SAED pattern are depicted in correct relative orientation to the TEM images and confirm that the long axis of the ZnO nanorods is parallel to the crystallographic [0001] direction.

whereas the particles formed after one and two minutes have been isolated and analyzed by TEM (Figure 3). After one minute of irradiation time, the sample contained uncoupled single hemi-rods and coupled rods, all characterized by rough surfaces (Figure 3a). In Figure 3a, it is also possible to observe two rods during the coupling process (marked with an arrow). The length of the coupled rods at this intermediate stage ranges between 280 and 512 nm, whereas the width varies between 94 and 205 nm, with a very narrow AR distribution between 2.5 and 3.12. The hemi-rods comprise lengths between 160 and 200 nm.

The sample isolated after two minutes of irradiation comprised coupled rods with length between 641 and 916 nm and width between 225 and 388 nm, the AR distribution being always very narrow (between 2.17 and 2.9). Therefore, longer reaction time led to longer and thicker rods, but the AR distribution kept almost constant. Furthermore, the surface of the rods isolated after two minutes appeared much more smooth, compared with rods found after one minute (Figure 3). A detailed SAED analysis was performed on ZnO nanorods isolated after one and two minutes reaction time, as shown in Figure 3b and d. Both SAED pattern were obtained in the region of the interface between the rod parts (marked by dotted circles in Figure 3b and d), which revealed that these regions are clearly single crystalline. Furthermore, from this SAED analysis, it is evident that the ZnO hemi-rods approached in [0002] direction towards each other before the attachment finally took place. To understand the attachment and formation mechanism in detail, a HRTEM analysis of single ZnO hemi-rods isolated after one minute reaction time was performed, as exemplarily shown in Figure 4a and b. It confirms that the surface of the hemi-rods is irregularly shaped and rough. Furthermore, the high-resolution TEM image in Figure 4b reveals that the hemi-rods, in which, for example, dislocations were observed, are defect-rich (see Figure S7 in the Supporting Information).

All these observations confirm that before the coupling process, the single hemi-rods exhibited at one side a rough defect-rich surface (basal plane) and oriented in [0001] direction towards each other. Finally, it can be concluded that the oriented attachment of single hemi-rods into one nanorod took place selectively through the rough and defect-rich basal planes. This conclusion is reasonable, because no hemi-rods that oriented to each other through the smooth surface parts were observed. Therefore, the seam cut is a clear evidence for the formation of a ZnO bicrystal arising from the aggregation of two hemi-rods along *c* direction and having a single-crystalline structure at the interface between the two rod parts as was confirmed by SAED.

Some control experiments have been carried out in the absence of DMF and PVP. Because the presence of the

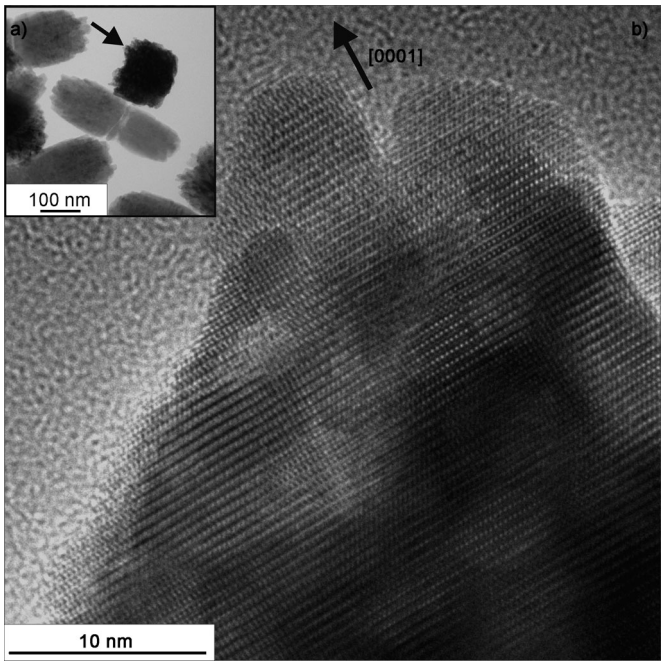

Figure 4. TEM analysis of ZnO hemi-rods isolated under MW irradiation after one minute; a) single and coupling hemi-rods are evident; b) HRTEM image acquired in the region marked with the arrow in a).

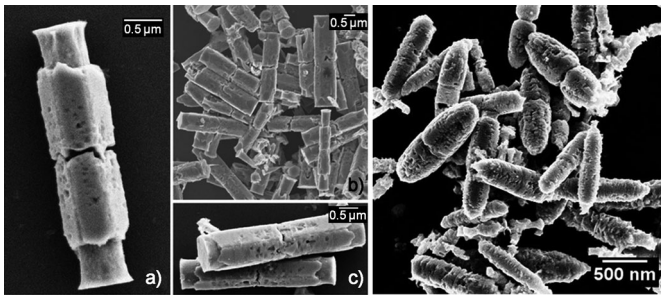

Figure 5. Seam-cut formation on ZnO micro- and nanorods under MW irradiation in the presence of an aqueous solution of NaOH according to the power, temperature profiles, and time presented in Figure S1 in the Supporting Information. a), b), c) particles synthesized in the absence of DMF; d) in the absence of PVP.

seam cut was evident in both structures, it can be concluded that neither DMF nor PVP are responsible for the formation of the seam cut, but rather NaOH and/or water (Figure 5 and the Supporting Information for experimental details).

Therefore, a scheme, in which a coupling process between two hemi-rods led to the formation of ZnO bicrystals can be drawn (Scheme 1). In fact, hemi-rods have been isolated after one minute of irradiation time and these building blocks have been found to undergo a coupling process along *c* axis leading to the formation of final single-crystalline ZnO bicrystals. Finally, dissolution and recrystallization led to the formation of rods with larger AR distribution (Scheme 1). To the best of our knowledge, this is the first

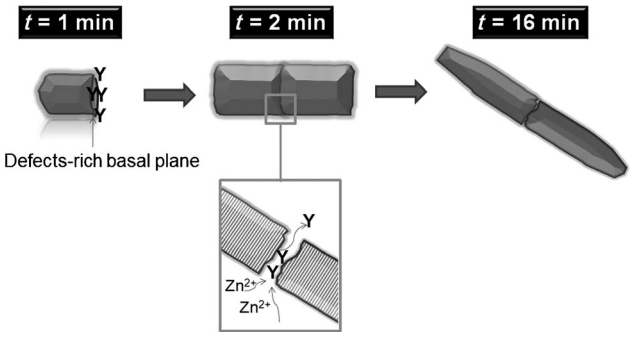

Scheme 1. Proposed mechanism for the formation of ZnO bicrystal nanorods under MW irradiation. Y indicates possible water and/or NaOH species adsorbed onto the interfaces.

time that through a kinetic study, the orientation of two hemi-rods along *c* axis under MW irradiation has been demonstrated, although similar bicrystal structures have been already reported.[8,9] We show clearly that the reason for the coupling can be ascribed to the high energy of the basal facets of the hemi-rods and that the presence of the seam cut is the consequence of a coupling process rather than etching due to pH.[13] The coupling through the smoother part of the rods has never been observed under our experimental conditions, whereas occasionally, multipods have been formed in the reaction mixture (Figures S2 and S3 in the Supporting Information).

In the present paper was demonstrate that under MW irradiation and in the presence of aqueous solution of NaOH, ZnO nanorods with a characteristic seam cut perpendicular to the elongation direction form. Although the rods at the seam cut are single crystalline, this microstructural feature is the consequence of a twinning process between ZnO hemi-rods that occurred by oriented attachment. In fact, highly reactive building blocks (hemi-rods) have been isolated after one minute and were observed by TEM. The hemi-rods possess a rough surface and are rich in defects at the basal plane (Figure 3a and b and Figure 4). The orientation occurred along *c* axis and only between rough and defect-rich interfaces. We believe that the driving force of the oriented attachment is the elimination of surfaces with high defect density through a coupling process of the single hemi-rods towards the formation of a single crystal. The determination of the nature of the interphases involved in the oriented attachment of the hemi-rods requires the assignment of the facets polarity.[14]

Experimental Section

In a typical experiment, a solution of PVP/$[Zn(O_2CCH_3)_2{\cdot}2H_2O]$ (3.75 mL, 0.01 g mL^{-1}, 0.025 M, respectively) was mixed with deionized water (7.5 mL) followed by addition of aqueous NaOH solution (3.75 mL, 0.013 M). After a ramp time of 3 min up to 200 °C, the reaction solution was allowed to react for 13 min (16 min sample). For the kinetic study, the reaction was stopped during the ramp time, when the working temperature of 200 °C was not yet reached (Figure S1 in the Supporting

Information). The instrument used for the synthesis was a LabMate™ device (CEM Corp., USA). SEM equipment used was a ULTRATM 55, Carl Zeiss AG, Germany. Conventional TEM and HRTEM were performed by using a Philips CM30 TWIN/STEM and a CM300 UltraTWIN, respectively. Both transmission-electron microscopes were operated by using a LaB6 filament at 300 kV acceleration voltage. For TEM investigations, the samples were dispersed in ethanol and dropped casted on commonly used copper grids coated with a continuous and holey carbon film. Electron-diffraction patterns were evaluated by using the software JEMS (version 3.6608U2011), incorporating the crystal data from the inorganic-crystal structure-data base (ICSD). The fast Fourier transformation analysis was performed by using the software DigitalMicrograph from Gatan Inc. XRD was performed by using a D8 advance instrument (Bruker AXS GmbH, Germany) with $Cu_{K\alpha}$ radiation ($\lambda = 1.5406$ Å) over a 2θ range from 10 to 80°. The samples for the analysis were prepared by casting the suspension of ZnO nanoparticles on the sample holders comprising low background sample cups with a vicinal (911) Si crystal of 25 mm diameter (Bruker AXS GmbH). TEM analysis and SAED of the sample isolated after 16 min showed that the interface between two ZnO rod parts is single crystalline and that the growth took place through *c* axis ([0001] direction; Figure 2a and corresponding inset). XRD evidenced that the final particles crystallized in wurtzite phase (Figure 2b), as was confirmed by SAED analysis (Figure 2a).

Acknowledgements

The authors gratefully acknowledge the support of the Cluster of Excellence "Engineering of Advanced Materials" at the University of Erlangen-Nuremberg, which is funded by the German Research Foundation (DFG) within the framework of its "Excellence Initiative".

Keywords: crystal polarity · interfaces · mesocrystals · microwave chemistry · nanostructures

[1] a) H. Cölfen, M. Antonietti, *Mesocrystals and Nonclassical Crystallization*, Wiley, Chichester, **2008**; b) D. Li, M. H. Nielsen, J. R. I. Lee, C. Frandsen, J. F. Banfield, J. J. De Yoreo, *Science* **2012**, *336*, 1014–1018.
[2] a) F. Banfield, S. A. Welch, H. Zhang, T. T. Ebert, R. L. Penn, *Science* **2000**, *289*, 751–754; b) A. P. Alivisatos, *Science* **2000**, *289*, 736–737.
[3] a) M. Distaso, R. Klupp Taylor, N. Taccardi, P. Wasserscheid, W. Peukert, *Chem. Eur. J.* **2011**, *17*, 2923–2930; b) M. Distaso, D. Segets, R. Wernet, R. Klupp Taylor, W. Peukert, *Nanoscale* **2012**, *4*, 864–873.
[4] X. Sun, X. Qiu, L. Li, G. Li, *Inorg. Chem.* **2008**, *47*, 4146–4152.
[5] F. Li, Y. Ding, P. Gao, X. Xin, L. Wang, *Angew. Chem.* **2004**, *116*, 5350–5354; *Angew. Chem. Int. Ed.* **2004**, *43*, 5238–5242.
[6] Y. Peng, A. W. Xu, B. Deng, M. Antonietti, H. Cölfen, *J. Phys. Chem. B* **2006**, *110*, 2988–2993.
[7] K. X. Yao, H. C. Zeng, *J. Phys. Chem. C* **2007**, *111*, 13301–13308.
[8] X. L. Hu, Y. J. Zhu, S. W. Wang, *Mater. Chem. Phys.* **2004**, *88*, 421–426.
[9] L. Zhang, Y. J. Zhu, *Appl. Phys. A* **2009**, *97*, 847–852.
[10] a) H. Y. Xu, H. Wang, Y. C. Zhang, S. Wang, M. K. Zhu, H. Yan, *Cryst. Res. Technol.* **2003**, *38*, 429–432; b) B. G. Wang, E. W. Shi, W. Z. Zhong, *Cryst. Res. Technol.* **1998**, *33*, 937–941; c) K. X. Yao, R. Sinclair, H. C. Zeng, *J. Phys. Chem. C* **2007**, *111*, 2032–2039.
[11] a) A. Taubert, D. Palms, Ö. Weiss, M. T. Piccinni, D. N. Batchelder, *Chem. Mater.* **2002**, *14*, 2594–2601; b) A. Taubert, C. Kübel, D. C. Martin, *J. Phys. Chem. B* **2003**, *107*, 2660–2666.
[12] a) H. F. Greer, W. Zhou, M. H. Liu, Y. H. Tseng, C. Y. Mou, *CrystEngComm* **2012**, *14*, 1247–1255; b) E. V. Rosseeva, J. Buder, P. Simon, U. Schwarz, O. V. Frank-Kamenetskaya, R. Kniep, *Chem. Mater.* **2008**, *20*, 6003–6013.
[13] S. C. Padmanabhan, D. Ledwith, S. C. Pillai, D. E. McCormack, J. M. Kelly, *J. Mater. Chem.* **2009**, *19*, 9250–9259.
[14] M. de La Mata, C. Magen, J. Gazquez, M. Iqbal Bakti Utama, M. Heiss, S. Lopatin, F. Furtmayr, C. J. Fernández-Rojas, B. Peng, J. Ramon Morante, R. Rurali, M. Eickhoff, A. Fontcuberta i Morral, Q. Xiong, J. Arbiol, *Nano Lett.* **2012**, *12*, 2579–2586.

Received: May 9, 2012
Published online: September 7, 2012

